

High-Temperature Lithiation of α -Fe₂O₃: A Mechanistic Study

M. M. THACKERAY*

*National Institute for Materials Research, CSIR, P.O. Box 395,
Pretoria 0001, South Africa*

W. I. F. DAVID

*Rutherford Appleton Laboratory, Chilton, Didcot, OX1 0QX,
United Kingdom*

AND J. B. GOODENOUGH

*Inorganic Chemistry Laboratory, South Parks Road, Oxford OX1 3QR,
United Kingdom*

Received February 7, 1984; in revised form June 4, 1984

The reaction mechanism for the lithiation of α -Fe₂O₃ has been studied at 420°C in electrochemical cells of the type Li-Al/LiCl, KCl/ α -Fe₂O₃. Initially the hexagonally close-packed oxide lattice transforms to cubic close-packed stacking. Electrochemical and structural data indicate that the discharge reaction proceeds via insertion of lithium into, and iron extrusion from, the cubic close-packed lattice to yield the final discharge products Li₂O and α -Fe. Previous reports have shown that this process is reversible and that high coulombic efficiencies can be obtained from this type of cell, provided that the electrode is not discharged to its full compositional limits. © 1984 Academic Press, Inc.

Introduction

Transition-metal oxides and chalcogenides have received considerable attention during the past decade as cathode materials for lithium batteries (1, 2). One system, in particular, that has received much interest as a possible high-energy/power-density battery for electric vehicles and for energy storage is the lithium-aluminum/LiCl, KCl/iron-disulfide system (3). This system, however, suffers from problems that can be related predominantly to the sulfide electrode, e.g., corrosion, and the high operating temperature of the battery (450°C). For this reason, a study of the electrochemical

performance of the less-corrosive iron oxides in a similar cell environment was undertaken recently (4, 5). In this investigation, it was demonstrated that both α -Fe₂O₃ and Fe₃O₄ cells showed good electrochemical characteristics in terms of electrode capacity, rechargeability, and lifetime. Similar behavior has also been observed using α -LiFeO₂ as cathode in these high-temperature cells (6).

In view of a recent report that lithium can be incorporated into α -Fe₂O₃ at ambient temperature (7), the structural characteristics of cathodes in high-temperature Li-Al/LiCl, KCl/ α -Fe₂O₃ cells have been reexamined. The results of this investigation are presented in this paper.

* To whom correspondence should be addressed.

Experimental

Electrochemical lithiation of α -Fe₂O₃ was undertaken in a cell of the form



The counter electrode consisted of a solid lithium-aluminum alloy, initially containing ~36% lithium. Cell voltages were monitored against a pure (>99.9%) magnesium reference electrode. The cathode consisted of 300 mg of α -Fe₂O₃ (Cerac, >99% pure, -325 mesh) compacted at 40 kN into a disk, 1 cm in diameter, and annealed at 700°C for 4 hr prior to use in the cell to obtain good mechanical strength. The pellet was contained in a sleeve of porous graphite felt and secured to the external circuit with molybdenum wire. The electrolyte consisted of a eutectic melt of LiCl (58^m%) and KCl (42^m%). The cell components were contained in a dense α -Al₂O₃ crucible. Cells were assembled and hermetically sealed under an argon atmosphere. The operating temperature was 420°C.

Cells were discharged galvanostatically at a constant current of 1 mA. Open-circuit voltages were obtained intermittently during discharge. Although equilibrium conditions were obtained in general after a few hours, cells were allowed to equilibrate for up to 24 hr.

Powder X-ray diffraction spectra of cathodes, after reaction at 420°C with 0.5, 1.5, 3.0, and 4.5 equivalents of lithium, were obtained at room temperature. In addition, a spectrum was obtained of a cathode that had been reacted with 4.5 equivalents of lithium and then recharged to a composition "Li_{0.4}Fe₂O₃." Cells were disassembled under an argon atmosphere to avoid contact of the electrodes with air. Samples were sealed from the atmosphere with a plastic spray. X-ray diffraction spectra were obtained from an automated Rigaku powder diffractometer that supplied CuK α radiation. The 2θ values were determined against an internal silicon standard.

Results and Discussion

The electrochemical reaction of lithium with α -Fe₂O₃ is presented in Fig. 1 in which the open-circuit voltage (o.c.v.) of the cell, with respect to the magnesium reference electrode, is plotted as a function of the number of reacting lithium atoms, x .

For $0 < x < 1.5$ it was apparent that the reaction proceeded by several steps involving single-phase and multiphase electrode processes; they are characterized in Fig. 1 by regions of decreasing voltage and of constant voltage, respectively. For $1.5 < x < 6.0$ the discharge curve is characterized by

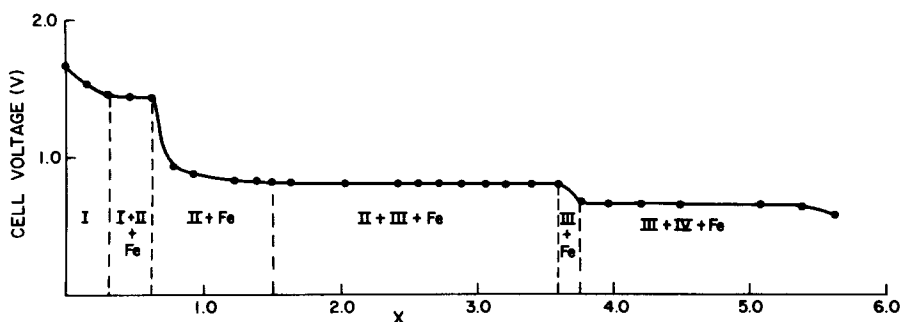


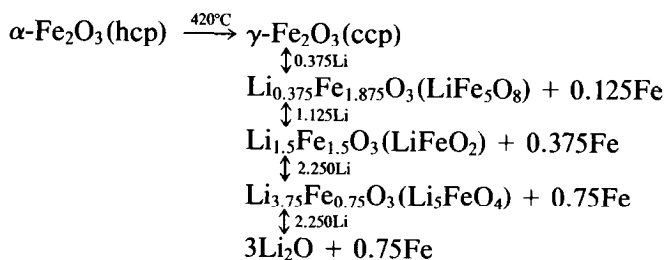
Fig. 1. Open-circuit voltage vs the number of reacting lithium atoms, x , in the high-temperature cell Mg/LiCl, KCl/ α -Fe₂O₃ at 420°C. The boundaries of the multiphase regions I + II + Fe and II + III + Fe depend on the history of the sample.

two distinct constant-voltage plateaus separated by 155 mV after reaction with 3.75 equivalents of lithium.

Although the room-temperature spectra of the lithiated iron-oxide cathodes do not reflect the exact situations that exist at the operating temperature of these cells, it was possible to extract important structural information regarding the nature of the reaction mechanisms. The spectra of the lithiated iron-oxide cathodes with $x = 0.5$, 1.5, and 3.0 were similar; all showed α -Fe and a cubic rock salt phase with an intensity distribution similar to that observed for α -LiFeO₂ (space group $Fm\bar{3}m$ (O_h^5)) (8). In α -LiFeO₂ all the octahedral sites of the cubic close-packed oxide lattice are occupied randomly by Li⁺ and Fe³⁺ ions. The refined "a" lattice parameter for the rock salt phase in each of these three cathodes was 4.164(2), 4.177(3), and 4.169(1) Å, respectively, compared to the literature value of 4.158 Å for α -LiFeO₂ (Li_{1.5}Fe_{1.5}O₃) (8). The powder spectrum of a cathode after reaction with 4.5 lithium equivalents, obtained after rapidly quenching the cathode to room temperature and immediately X-raying the

sample, was characterized by α -Fe, α -Li₅FeO₄, and Li₂O. The spectrum of a cathode that had been reacted with 4.5 lithium equivalents and then recharged to a hypothetical composition "Li_{0.4}Fe₂O₃" showed a two-phase product consisting of a rock salt phase ("a" = 4.232(1) Å), as described above, and a cubic spinel-type phase ("a" = 8.399(1) Å). This spectrum is shown in Fig. 2. It was apparent from this spectrum that the free iron, extruded during discharge, had been reabsorbed into the oxide lattice while charging the cell. Although only the strongest reflections were evident, the intensity distribution suggested a spinel-type phase intermediate between γ -Fe₂O₃ (9) and LiFe₅O₈ (10), indicative of tetrahedral-site occupation by the ferric cations.

If the reaction were characterized by a continuous insertion of lithium into, and iron extrusion from, the cubic close-packed oxide lattice, it would be possible to characterize every phase of the cathode during the reaction by the compound Li_xFe_{2-x/3}O₃ for $0 < x < 6$. The reaction sequence could thus be represented by



This is the reaction sequence proposed by Godshall (11) in a thermodynamic study of the ternary Li-Fe-O system at 400°C. However, in our experiments there is evidence that the thermodynamically stable system is reached in two steps, one fast and the other slow; and it appears that the slow

step is not completed in our experiments, at least on initial discharge.

In particular, the electrochemical curve in Fig. 1 suggests that, for $0 < x < 1.5$, lithiation of α -Fe₂O₃ to Li_xFe₂O₃ occurs by several stages involving both single-phase and multiphase electrode processes. A flat

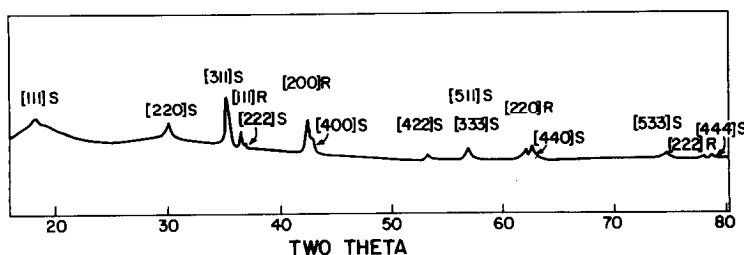


FIG. 2. The X-ray diffraction spectrum of " $\text{Li}_{0.4}\text{Fe}_2\text{O}_3$ " showing the two-phase nature of the cathode, where S = spinel phase and R = rock salt phase. The LiCl, KCl electrolyte and Si standard peaks have been omitted from the figure for clarity.

V_{oc} versus x curve at $x = 0.375$ indicates that the spinel composition LiFe_5O_8 is in a multiphase region in the initial discharge. On the other hand, the phase Li_3FeO_4 near $x = 3.75$ is clearly marked; but the plateaus either side of $x = 3.75$ are separated by 155 mV in our case whereas Godshall *et al.* report only a 26-mV separation after a shorter equilibration time (6).

Conversion of $\alpha\text{-Fe}_2\text{O}_3$ to $\gamma\text{-Fe}_2\text{O}_3$: Li on initial lithiation allows for rapid Li insertion into the octahedral vacancies of the spinel phase over the range $0 < x \leq 0.25$ to give the end-member spinel $\text{Fe}_{8/3}\text{Li}_{1/3}\text{O}_4$. (Note that x is everywhere referred to three oxide ions.) The initial single-phase region (I), where $V_{oc} = V_{oc}(x)$ in Fig. 1, corresponds roughly to this range if account is taken of the nonuniformity of the Li-insertion process in the polycrystalline cathodes. (The shape of the discharge curve in the compositional range $0 < x < 1.5$ depended upon the procedure of cathode fabrication.) However, this fast reaction is, in principle, followed by a slow disproportionation reaction



that involves the extrusion of $\alpha\text{-Fe}$. If the second reaction goes to completion, the end-member spinel is LiFe_5O_8 . It would appear that extrusion of iron occurs at the particle surfaces in our experiments, but probably does not occur throughout the bulk of the particles. Our spinel phases un-

doubtedly contain some Fe^{2+} ions, which makes them formally a member of the solid-solution system $\text{Li}_y\text{Fe}_{3-y}\text{O}_4$ in the composition range $0.33 \leq y \leq 0.5$ or $0.25 \leq x \leq 0.375$. In Fig. 1, phase I is the spinel $\square_z\text{Li}_y\text{Fe}_{3-y-z}\text{O}_4$, where z depends on the extent of iron extrusion as well as on y .

Lithiation beyond the end-member spinel phase $\text{Fe}[\text{Fe}_{2-y_c}\text{Li}_{y_c}]\text{O}_4$, where $0.33 < y_c < 0.5$ corresponds to $0.25 < x_c < 0.375$, occurs via insertion of Li^+ ions into the interstitial octahedral sites of the spinel phase. In a cubic spinel these are the $16c$ sites of the space group $Fd\bar{3}m$. Electrostatic forces between the Li^+ ions in sites $16c$ and the tetrahedral-site Fe^{3+} ions in positions $8a$, with which they share common site faces, would displace the Fe^{3+} ions to neighboring $16c$ sites. Such a process results in a cation-deficient rock salt structure in which the octahedral $16c$ and $16d$ positions of the space group $Fd\bar{3}m$ remain distinguishable (7):



However, between the stable compositional range for this phase (II) and the spinel phase there is a multiphase region I + II + Fe. From Fig. 1, the multiphase boundary extends to $x \approx 0.66$ or $y \approx 0.88$, so the rock salt phase that is established on the disappearance of the spinel phase is, roughly,



if the limiting spinel phase LiFe_5O_8 is reached in the initial step. Further lithiation introduces Li^+ ions into the octahedral-site vacancies \square in a relatively fast step; this insertion reaction may be followed by a slower disproportionation reaction. The compositional regions in which $V_{\text{oc}}(x)$ has a small variation with x correspond to regions where further lithiation depends upon extrusion of metallic iron. The limiting composition for this process is $\text{Li}_2\text{Fe}_2\text{O}_4$ or LiFeO_2 . It should be noted that after the fast step, the rock salt phase contains Fe^{2+} ions, and the lattice parameter of the rock salt phase depends sensitively on the Li/Fe^{2+} ratio. Where Fe^0 extrusion is incomplete, the lattice parameter is larger than the $a_0 = 4.158 \text{ \AA}$ for $\alpha\text{-LiFeO}_2$. Comparison of the lattice parameter for $\alpha\text{-LiFeO}_2$ with a measured " a " $\approx 4.17 \text{ \AA}$ for the rock salt phase obtained on lithiation during the first discharge cycle indicates that the concentration of Fe^{2+} ions in this phase is relatively small for $x \geq 0.5$. On the other hand, recharging to $x = 0.4$ gives a rock salt phase with " a " $= 4.23 \text{ \AA}$, which is indicative of a more significant Fe^{2+} -ion concentration in phase II associated with the incorporation of extruded Fe^0 into the oxide lattice. This finding suggests that the concentration of Fe^{2+} ions that may be stabilized in the rock salt structure at 400°C depends upon the history of the sample. The same should also be true of the spinel phase $\text{Li}_y\text{Fe}_{3-y}\text{O}_4$ (I) with which it coexists in the multiphase region. Finally, the difference between room-temperature lithiation of $\alpha\text{-Fe}_2\text{O}_3$ and that at 420°C is the rate and extent to which the slow reaction proceeds over the lifetime of an experiment. The rock salt product obtained for $x = 1$ in the room-temperature lithiation $\text{Li}_x\text{Fe}_2\text{O}_3$ approaches the value expected for no extrusion of iron (see Fig. 3).

Lithium in excess of $x = 1.5$ requires either the introduction of ions into tetrahedral sites or the oxidation of iron to Fe^{4+} in

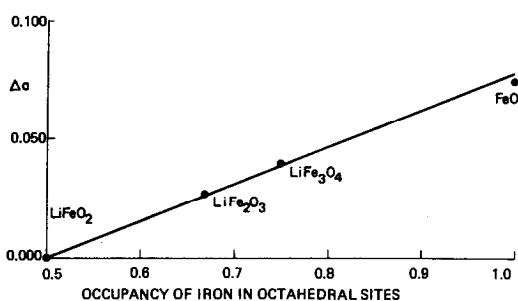


FIG. 3. Variation of the unit cell length per cubic close-packed oxygen atom (Δa) of LiFeO_2 , LiFe_2O_3 , LiFe_3O_4 , and FeO with iron occupancy in octahedral sites.

the disproportionation reaction. The latter alternative is not possible, and displacement of ions into tetrahedral sites produces new phases: Li_3FeO_4 (III) and Li_2O (IV). In the end-member Li_2O , all the tetrahedral sites are occupied. In the Li_3FeO_4 intermediate, an ordered occupation of tetrahedral sites by ferric ions results in a lowering of the crystal symmetry from cubic to orthorhombic (12).

Three features of this reaction mechanism should be highlighted. First, during discharge lithium is inserted into, and iron extruded from, a cubic close-packed oxide lattice that, for certain composition ranges, becomes distorted; this process is reversible. Second, for $0 < x < 1.5$, lithiation of $\gamma\text{-Fe}_2\text{O}_3$ (spinel) to yield $\alpha\text{-LiFeO}_2$ (rock salt) results in complete occupation of the octahedral sites of the structure. The volume of the oxide lattice, based on room-temperature unit-cell data, decreases by 0.86%. For $1.5 < x < 6.0$, cations migrate from octahedra to tetrahedra; the increase in volume associated with the $\alpha\text{-LiFeO}_2$ to Li_2O transition is massive: 36.41%. Third, the limited solubility of the lithium-iron-oxide phases in the molten LiCl , KCl electrolyte accounts for the good coulombic efficiencies and lifetimes reported earlier for this type of cell (5). Only on deep discharge, with the generation of Li_2O and its slow dispersion

into the electrolyte, does a gradual deterioration in cell performance occur.

It is worthwhile to compare these results with those obtained from a recent study of the lithiation of α -Fe₂O₃ and Fe₃O₄ at ambient temperature (7). Reaction with *n*-butyllithium at 50°C yielded cubic Li_{*x*}Fe₂O₃ ($x < 1.7$, “*a*” = 8.422 Å) and Li_{*x*}Fe₃O₄ ($x < 1.5$, “*a*” = 8.474 Å). At $x = 1$ all the octahedral sites of the cubic close-packed oxide lattice are occupied by lithium and iron. Lithium ions in excess of $x = 1.0$ must occupy tetrahedra sharing faces with octahedra. Not surprisingly, therefore, compounds with $x > 1$ were observed to be unstable and tended to ignite in air, particularly for high values of x . This was attributed to lithium diffusion from the bulk of a particle back to the surface where oxidation of metallic lithium readily occurs (13). In view of the disclosure that traces of “unreacted iron oxide” were present after reaction with *n*-butyllithium (7) and particularly on account of the results of the present investigation, it appears that in the cell finely divided iron is slowly extruded from the lattice to accommodate lithium in excess of $x = 1$; on withdrawal from the *n*-butyllithium solution, Li⁺ ions are rapidly extruded to the surface. Both lithium and iron on the surface are readily oxidized when exposed to air. Lithiation in excess of $x = 1$ of at least the smaller particles of Li_{*x*}Fe₂O₃ was also indicated by a slight asymmetry of the peaks toward higher 2θ values in the X-ray spectrum of “Li_{1.7}Fe₂O₃”; this asymmetry can be attributed to concentration gradients of the iron ions in the individual particles. If iron extrusion had not reached equilibrium, the surface of the particles after Li insertion would be less rich in iron (i.e., closer to LiFeO₂) and hence have the smaller lattice parameter as observed (7).

Structural analysis of Li_{*x*}Fe₂O₃ and Li_{*x*}Fe₃O₄, prepared with *n*-butyllithium, revealed that the former compound has predominant rock salt-like characteristics.

Li_{*x*}Fe₃O₄ was characterized by a structure in which the [Fe₂]O₄ framework of the Fe_{tet}[Fe₂]_{oct}O₄ spinel was retained during lithiation; the other cations, at $x = 1$, randomly occupy the remaining octahedral sites. A plot of the variation of the “*a*” lattice parameter per oxygen atom of the rock salt phases LiFeO₂, LiFe₂O₃, Fe_{1- δ} O, and the partially ordered rock salt phase LiFe₃O₄ vs the iron occupancy in octahedral sites yields, at a first approximation, a linear relationship (Fig. 3).

Finally, a comment about the influence of the mobilities of the lithium and iron ions on structure: synthesis of α -LiFeO₂ at high temperature (typically 900°C), where both lithium and iron are highly mobile, generates a true rock salt phase in which all the octahedral sites of the cubic close-packed oxide lattice are occupied randomly by Li⁺ and Fe³⁺ ions. In contrast, the ionic mobilities of these cations, particularly iron, are appreciably lower at 50°C; chemical lithiation of α -Fe₂O₃ causes the hexagonally close-packed oxide lattice to shear to cubic close-packed stacking and results in a rock salt-like structure at Li_{1.0}Fe₂O₃ in which all the octahedral sites of the oxide lattice are occupied, but with a distribution of iron that slightly favors the *B* octahedral sites of an A[B₂]O₄ spinel (7).

Acknowledgments

Financial assistance from the South African Inventions Development Corporation is gratefully acknowledged.

References

1. G. PISTOIA, *J. Power Sources* **9**, 307 (1983).
2. M. S. WHITTINGHAM, *Prog. Solid State Chem.* **12**, 41 (1978).
3. R. K. STEUNENBERG, in “Fast Ion Transport in Solids” (P. D. Vashishta, J. N. Mundy, and G. K. Shenoy Eds.), p. 23, Elsevier, Amsterdam (1979).
4. M. M. THACKERAY AND J. COETZER, S.A. patent 80/6497.

5. M. M. THACKERAY AND J. COETZER, *Mater. Res. Bull.* **16**, 591 (1981).
6. N. A. GODSHALL, I. D. RAISTRICK, AND R. A. HUGGINS, *Mater. Res. Bull.* **15**, 561 (1980).
7. M. M. THACKERAY, W. I. F. DAVID, AND J. B. GOODENOUGH, *Mater. Res. Bull.* **17**, 785 (1982).
8. ASTM Powder Diffraction File 17-938.
9. ASTM Powder Diffraction File 25-1402.
10. ASTM Powder Diffraction File 17-115.
11. N. A. GODSHALL, Dissertation thesis, Stanford University, Stanford, Calif., June (1980).
12. G. DEMOISSON, F. JEANNOT, C. GLEITZER, AND J. AUBRY, *C.R. Acad. Sci. Paris, Ser. C* **272**, 458 (1971).
13. M. M. THACKERAY, W. I. F. DAVID, P. G. BRUCE, AND J. B. GOODENOUGH, *Mater. Res. Bull.* **18**, 461 (1983).